Proceedings of 20th International Congress on Acoustics, ICA 2010

23-27 August 2010, Sydney, Australia

Linear stability analysis applied to flow duct acoustics

Mikael Karlsson[1] and Mats Åbom[2]

(1) KTH Cicero, The Marcus Wallenberg Laboratory for Sound and Vibration Research, Stockholm, Sweden
(2) KTH, Linné Flow Centre, Stockholm, Sweden

PACS: 43.28 Py, 43.28 Ra

ABSTRACT

Linear stability analysis is applied to configurations based on a T-junction subjected to grazing flow. This setup is a well-known case where flow-acoustic interaction can result in aperture tones provided sufficient acoustic feedback is present. The flow acoustic interaction is characterised as Rayleigh impedances, these together with the acoustic impedance of the attached components result in a total impedance that characterises the system. Stability analysis is then applied to the derived total impedance using a slightly modified version of the Nyquist criterion as known from control theory.

INTRODUCTION

Flow-acoustic interaction in flow duct systems could lead to intense noise, often denoted a whistle, which not only could be disturbing but also could lead to mechanical failure of the structure. Full simulations of a typical system such as a gas pipelines or automotive exhaust/intake systems are still too computationally expensive to be viable. A common simplification of the problem is to divide the system into a network of linear acoustic multiports. Each of these "black boxes" could then be determined analytically, numerically or experimentally. This approach is widely used for studying passive system properties such as reflection and transmission of sound.

It has been shown, Karlsson and Åbom [1], that flow-acoustic coupling effects could be included in the linear multi-port, that is, it can act as an amplifier. For a given amplification rate one can then determine whether the linear network is stable or not [2]. This type of analysis is common practise in the design of RF and MW circuits [3].

Here the linear stability analysis will be applied to study potential whistling from a T-Junction subjected to grazing flow. Vorticity within the shear layer interacts with the acoustic field while being convected across the orifice. The interaction can be constructive or deconstructive depending on the Strouhal number (relating the travel time of the vorticity with the acoustic period). If the sufficient acoustic feedback is given to the amplifier the response becomes non-linear, resulting in a self-sustained oscillation (whistle). The shear layer then tend to roll up in discrete vortices. Given that the data collapse with a Strouhal number based on the convection velocity of the vorticity/vortices, which is not influenced by their strength, it is sufficient to study the linear system to find the instability frequencies (Howe [4]).

The flow-acoustic coupling will be characterised via a quantity denoted the Rayleigh impedance, see Howe [5], which in turn is derived from the system matrix. The total system response is then given by the Rayleigh impedance and the impedance given by the acoustic system it is coupled to. There are various means to perform the stability analysis. Here the Nyquist stability criteria will be used. It is basically an implementation of Cauchy's principle of the argument and provides an graphical tool to search for poles or zeros in the unstable halfplane of a complex function. A similar approach was presented by Sattelmayer and Polifke [6] for thermo-acoustic instabilities.

THEORY

Active acoustic threeport

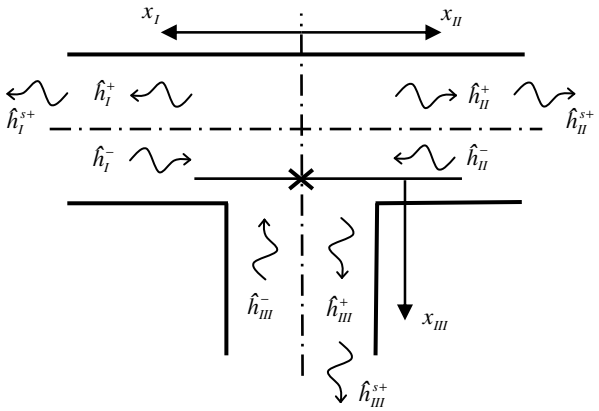

Figure 1. Three port definition.

The T-Junction will be represented as an active acoustic three-port, see Figure 1. The three-port is reduced to a single point, marked with a bold X in Figure 1, which is placed along the centre line of the side branch a distance into the main duct given by the end correction without flow [7]. Assuming the system to be linear and time invariant and choosing the scattering matrix form it can be represented as:

$$\hat{\mathbf{h}}_+ = \mathbf{S}\hat{\mathbf{h}}_- + \hat{\mathbf{h}}^{s+} \qquad (1)$$

Where $h' = p'/\rho_0 + U_0 u'$ is the acoustic stagnation enthalpy and the superscript *s* indicates an uncorrelated source term. Any correlated modulation of the sound by flow-acoustic interaction must then be included in the scattering matrix **S** [1]. It then consists of two parts:

$$\hat{\mathbf{h}}_+ = (\mathbf{S}_0 + \mathbf{S}_m)\hat{\mathbf{h}}_- + \hat{\mathbf{h}}_0^{s+} \qquad (2)$$

Where the subscript zero indicates the scattering properties of the system without flow modulation and subscript *m* indicates the part given by the modulation. In experimentally determined data, as will be used here, one cannot distinguish between the two. That is, flow-acoustic interaction effects are included in the measured scattering matrix.

The experimental setup and methodology used for determining the scattering matrix and source vector is described in [1] and will not be further discussed here.

Whistling potentiality

Having access to the system scattering matrix one can find the regions where the three-port amplifies incoming sound by performing a power balance. Exciting one branch at the time and assuming the two branches not excited as being anechoic the following power balances are found:

$$\frac{\langle P_I^{out} \rangle}{\langle P_I^{in} \rangle} = \frac{|R_I|^2 A_I + |T_{I-II}|^2 A_{II} + |T_{I-III}|^2 A_{III}}{A_I} \qquad (3)$$

$$\frac{\langle P_{II}^{out} \rangle}{\langle P_{II}^{in} \rangle} = \frac{|T_{II-I}|^2 A_I + |R_{II}|^2 A_{II} + |T_{II-III}|^2 A_{III}}{A_{II}} \qquad (4)$$

$$\frac{\langle P_{III}^{out} \rangle}{\langle P_{III}^{in} \rangle} = \frac{|T_{III-I}|^2 A_I + |T_{III-II}|^2 A_{II} + |R_{III}|^2 A_{III}}{A_{III}} \qquad (5)$$

Where *R* and *T* are the reflection and transmission coefficients from the scattering matrix in Eq.(1) and *A* is the cross sectional area. This only provides information under which conditions the system amplify or attenuate an incident acoustic wave. Here this information will be used to design the resonators used to potentially make the system sustaining an oscillation.

Rayleigh impedance

It has been shown that system stability can be predicted accurately with an approach using the full three-port [2]. The reason for reducing the available data into a Rayleigh impedance is simply an attempt to find a quantity which can yield some further insight in the involved physics. The Rayleigh impedance is here defiend as:

$$Z_R = \frac{\hat{h}_{I,II} - \hat{h}_{III}}{\hat{m}_{side}} \qquad (6)$$

Where $m' = (\rho_0 u' + \rho' U_0)A$ is the acoustic mass flow and the subscript *I,II* indicates a point in the main duct above the orifice. The real part of the Rayleigh impedance (resistance) can be seen as a measure of the interchange of energy in between the acoustic and hydrodynamic field where a negative resistane can indicate sound amplification [8]. The imaginary part of the Rayleigh impedance (reactance) can be seen as a change in the apparent mass of the orifice. This is commonly interpreted as an end correction.

Now, for the system to become unstable the Rayleigh impedance must overcome the radiation impedance seen in the connecting branches. This can be seen as computing the eigenfrequencies of the system. The passive terminations can be related to the state variables as:

$$\begin{cases} \hat{h}_{I,II} = -\hat{m}_{III} \dfrac{1}{\dfrac{1}{Z_I} + \dfrac{1}{Z_{II}}} \\ \hat{h}_{I,II} = \hat{m}_{III} Z_{III} \end{cases} \qquad (7)$$

Which, when inserted into Eq. (6) yields:

$$\underbrace{\left(\frac{1}{\dfrac{1}{Z_I} + \dfrac{1}{Z_{II}}} + Z_{III} + Z_R \right)}_{Z} \hat{m}_{III} = 0 \qquad (8)$$

Where *Z* is the total system impedance to which the stability analysis can be applied. However, unlike the ideal case discussed by Howe [5] (a single hole with the acoustic propagation restriced to the main axis of the hole and backing cavity) the response of the shear layer in the T-Junction discussed here will be dependent upon the combined excitation of all three branches. To compensate for this the Rayleigh impedance will be divided into three components, one representing each branch.

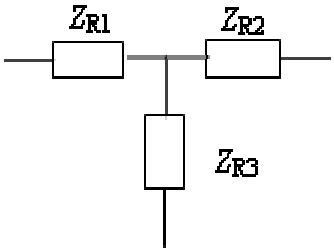

Figure 2. Representation of the flow-acoustic interaction in the T-Junction via Rayleigh impedances.

Starting from the impedance formulations given in [1] ($Z_{\text{I-III}}$, $Z_{\text{II-III}}$ and Z_{III}), which represent the impedance given by excitation from one port at the time (with the other two ports anechoic) and going into the side branch, expressions for Z_{RI}, Z_{RII} and Z_{RIII} can be derived.

$$Z_{I-III} = 1 + Z_{RI} + Z_{RIII} + \frac{Z_{RI}(1 + Z_{RIII})}{1 + Z_{RII}} \qquad (9)$$

$$Z_{II-III} = 1 + Z_{RII} + Z_{RIII} + \frac{Z_{RII}(1 + Z_{RIII})}{1 + Z_{RI}} \qquad (10)$$

$$Z_{III} = Z_{RIII} + \frac{1}{\dfrac{1}{1 + Z_{RI}} + \dfrac{1}{1 + Z_{RII}}} \qquad (11)$$

This result in a non linear set of equations, but assuming second order terms are small one can solve iteratively. Rearranging one arrive at:

$$\begin{pmatrix} -2 & (Z_{I-III}-1) & -1 \\ (Z_{II-III}-1) & -2 & -1 \\ (Z_{III}-1) & (Z_{III}-1) & -2 \end{pmatrix} \begin{pmatrix} Z_{RI} \\ Z_{RII} \\ Z_{RIII} \end{pmatrix}_{n+1} = \begin{pmatrix} 1+Z_R^2-Z_{I-III} \\ 1+Z_R^2-Z_{II-III} \\ 1+Z_R^2-2Z_{III} \end{pmatrix}_n \quad (12)$$

Where n is the iteration number and

$$Z_R^2 = Z_{RI}Z_{RII} + Z_{RI}Z_{RIII} + Z_{RII}Z_{RIII}$$

Having obtained the three Rayleigh impedances Eq. (8) should be updated to:

$$\underbrace{\left(\frac{1}{\frac{1}{Z_I+Z_{RI}} + \frac{1}{Z_{II}+Z_{RII}}} + Z_{III} + Z_{RIII} \right)}_{Z} \hat{m}_{III} = 0 \quad (13)$$

Linear stability – Nyquist plot

Now having derived the impedance Z that characterises the system (including the terminations) one can start looking for instabilities. Eq. (13) has non trivial solution (eigenfrequencies) when Z=0. If these zeros are in the unstable halfplane they will result in exponentially growing modes.

There are various ways of searching for the poles and zeros of a complex function. One appealing version is the Nyquist criterion which basically is an implementation of Cauchy's principle of the argument which yields the number of poles or zeros inside an contour in the complex frequency plane. In practise data is only available along the positive real axis. However, assuming the system to be causal and vanishing for large ω and also noting that zeros/poles occur in pairs, that is, for a zero/pole with positive real part there will exist a corresponding one at -ω*, implies that it is sufficient to study the positive real axis. This will create a clockwise contour covering the critical lower half plane (assuming the Fourier transform is defined using exp(-$i\omega t$)).

The application of this is the Nyquist plot where the number of encirclement around the critical point (0,i0) in the complex Z(ω)-plane is a measure of the number of zeros/poles in the lower half plane. If the encirclements are clockwise it indicates zeros and vice versa for poles.

TEST CASES

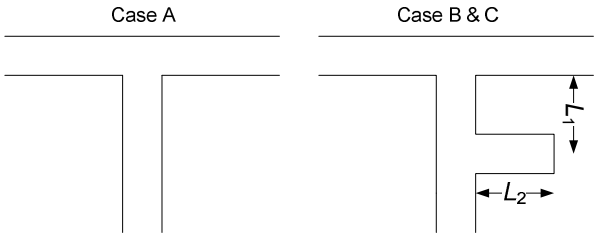

Figure 3. Schematic of test cases.

The stability analysis will be applied to three cases. They are all based on the same base setup, then only the impedance in the side branch is changed. This is realised by the two setups shown in Figure 3. First straight cylindrical ducts (d=0.057 m) are attached to all three ports (Case A). This is actually the setup used for determining the scattering matrix **S** [1], hence care has to be taken to reduce the reflection from the termination to ensure a linear response. From this first case the reflections (and consequently the impedances) in all three terminations are known. Secondly, a resonator arrangement is replacing the straight duct attached to the side branch. That is, for Case B & C all impedances in Eq. (13) remain unchanged from case A except for Z_{III}. The resonator arrangement is tuned, by changing the lengths L_1 and L_2, to provide maximum acoustic feedback at frequencies where the system act as an amplifier (identified via the power balances given by Eqs. (3-5)). The diameter of the ducts in the resonator arrangement equals the diameter of the main ducts. In all configurations the mean Mach number of the incident flow is 0.15.

RESULTS

From the known scattering matrix for the T-junction the Rayleigh impedances of the three duct are derived using the procedure of Eq. (12), see Figure 4. It is clear that the flow acoustic interaction is most significant with sound incident from Branch III. This is in line with expectation from the commonly excepted explanation model of the phenomenon [9]. Less expected is the fact that the Rayleigh impedance in Branch II display distinct regions with negative resistance and Branch I to less degree. This is opposite to previous experience and—as will be seen next—neither do it agree with the results from the power balance procedure.

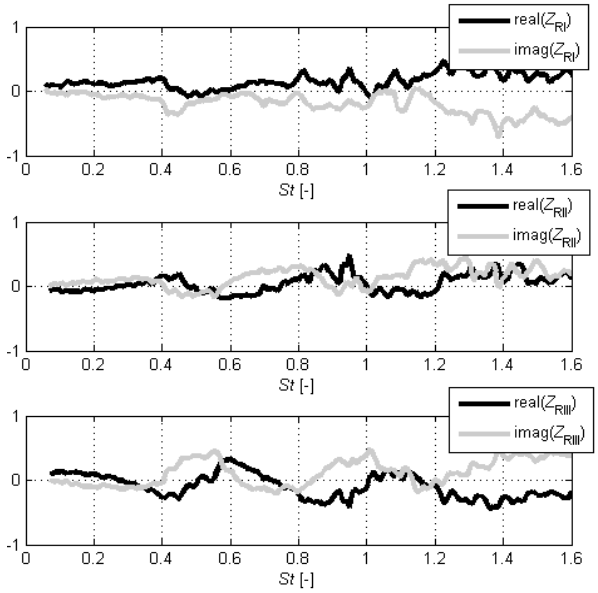

Figure 4. Rayleigh impedances in the three branches.

Now, to design the resonator of cases B & C the power balance procedure of Eqs. (3-5) is used where a value larger than unity indicate sound amplification. Again, see Figure 5, incient sound from Branch III clearly triggers the flow acoustic interaction; alternating region of positive and negative power is seen. This, and the fact that there is no mean flow in this branch was the motivation for placing the resonator arrangement there. The arrangement is then tuned towards the amplification peaks for the side branch, that is, Strouhal numbers of 0.45 (Case B) and 0.9 (Case C) respectively. In this setup is corresponds to 510 and 1020 Hz. It is of interest to compare the power balance for a sound incident from the up and down stream duct to the corresponding Rayleigh imedances. Here it is the upstream excitation that result in a stronger amplification.

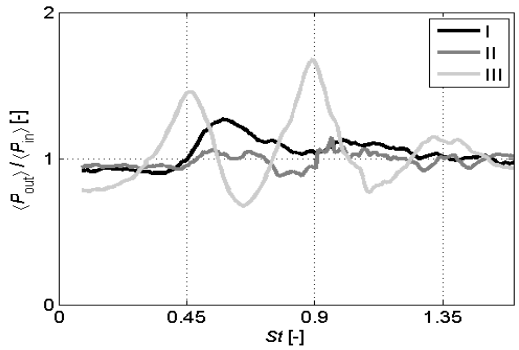

Figure 5. Power balances according to Eqs. (3-5).

Now, having determined the Rayleigh impedances and the test setups, the linear stability check according to Eq. (13) can be performed. The results for the two resonator arrangements are seen in Figure 6. The resonator tuned towards *St*=0.45 do not encircle the critical point (0,0i) and should be stable. The other resonator arrangement display two clockwise encirclements around the critical point. One which is at the targeted frequency and one which is just below at *St*=0.84. That is, there are two instability frequencies relatively close to each other. The result for Case A is not shown here but it is predicted stable. This is of course most important since the determination of the scattering matrix would fail otherwise.

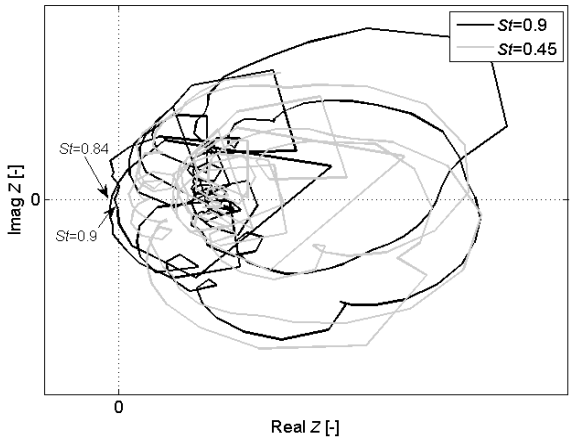

Figure 6. Linear stability check of Case B & C.

In Figure 7 the three cases are tested experimentally. The quantity shown corresponds to the source term in Eq. (2). As was predicted by the stability anlysis are Case A & B stable while case C displays a distinct tone at *St*=0.9. However, there is only a single tone, not another one at *St*=0.84 as well. It can be argued that "lock-in" effects would result in a single tone even though there are multiple instability frequencies in a narrow range [10]. However, it has been shown that using a more complete formulation of the problem—where the system response is not reduced to three impedances—that one can distuingish in between the instability frequencies [2].

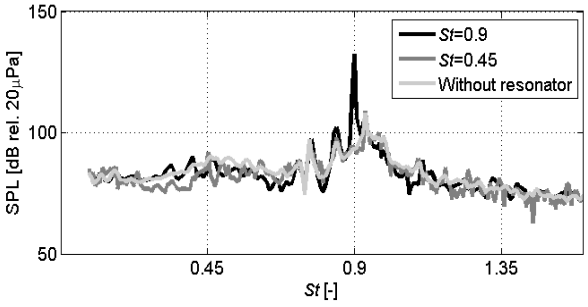

Figure 7. Source term according to Eq.(1) for all three cases.

DISCUSSION

It has been shown previously that a linear stability analysis works for predicting the whistling frequencies of a system including flow-acoustic coupling. In this work the more complete formulation of [2] was compared with an approach where the flow acoustic interaction was represented by Rayleigh impedances, The reason for this is to get a qunatitiy which could yield some insight in the flow acoustic interaction. The approach successfully determined which configuration whistles and which that does not. It also predicted the frequency of the whistle, however, it also came up with another potential instability close to the first one. In practise it can be discussed if one could separate in between the two in a validation measurement.

The reason that the second instability frequency appeared is likely to be due to the reduction of the system matrix into three impedances. Here it was performed starting from an reduced set of data. To improve the result the Rayleigh impedances should be derived in a more rigorous manner including all the components of the system scattering matrix.

ACKNOWLEGDEMENTS

The financial support of the Swedish Energy Agency, Project 32022-1, is kindly acknowledged.

REFERENCES

1 M. Karlsson, and M. Åbom, "Aeroacoustics of T-junctions-an experimental study", *Journal of Sound and Vibration*, Vol. 329, 1793-1808, (2010),

2 M. Karlsson, and M. Åbom, "On the use of linear aeroacoustic methods to predict whistling", Submitted

3 G. D. Vendelin, A. M. Pavio, and U. L. Rohde, *Microwave circuit design using linear and nonlinear techniques*, (Wiley, Hoboken New Jersey, 2005)

4 M. S. Howe, "Edge, cavity and aperture tones at very low Mach numbers", *Journal of Fluid Mechanics*, Vol. 330, 61-84, (1997),

5 M. S. Howe, *Acoustics of Fluid-Structure Interactions*, (Cambridge University Press, Cambridge, 1998)

6 T. Sattelmayer, and W. Polifke, "A novel method for the computation of the linear stability of combustors", *Combustion Science and Technology*, Vol. 175, 477-497, (2003),

7 V. Dubos, J. Kergomard, A. Khettabi, J. P. Dalmont, D. H. Keefe, and C. J. Nederveen, "Theory of Sound Propagation in a Duct with a Branched Tube Using Modal Decomposition", *Acta Acustica*, Vol. 85, 153-169, (1999),

8 J. W. Coltman, "Sounding Mechanism of the Flute and Organ Pipe", *Journal of the Acoustical Society of America*, Vol. 44, 983-992, (1968),

9 P. A. Nelson, N. A. Halliwell, and P. E. Doak, "Fluid dynamics of a flow excited resonance, Part II: Flow acoustic interaction", *Journal of Sound and Vibration*, Vol. 91, 375-402, (1983),

10 H. R. Graf, and S. Ziada, "Excitation source of a side-branch shear layer", *Journal of Sound and Vibration*, Vol. 329, 2825-2842, (2010),